Harmonic oscillators in relativistic quantum mechanics

F. M. Toyama[1,*] and Y. Nogami[2]
[1]*Department of Information and Communication Sciences, Kyoto Sangyo University, Kyoto 603-8555, Japan*
[2]*Department of Physics and Astronomy, McMaster University, Hamilton, Ontario, Canada L8S 4M1*
(Received 14 August 1998; revised manuscript received 16 October 1998)

For the Dirac equation in one space dimension, we examine the possibility of harmonic oscillator (HO) potentials. A HO potential is such that it has only bound states and the energy levels are equally spaced. Regarding their Lorentz transformation properties, there are three types of potentials for the Dirac equation: vector, scalar, and pseudoscalar. HO potentials are possible for the scalar and pseudoscalar types, but not for the vector type. We show how HO potentials can be constructed by means of the ''inverse scattering method.'' We also examine the behavior of a wave packet in the HO potentials so constructed. The behavior is, in most of the cases, very similar to that of Schrödinger's coherent wave packet of the nonrelativistic harmonic oscillator. [S1050-2947(99)09802-9]

PACS number(s): 03.65.Pm

I. INTRODUCTION

The harmonic oscillator (HO) is one of the most basic and useful solvable examples in nonrelativistic quantum mechanics with the Schrödinger equation. Among many of its features, let us focus on the following two. (i) The HO has an infinite number of bound states whose energies are all equally spaced. (ii) The HO accommodates a coherent wave packet that oscillates exactly like its classical counterpart and its shape (in terms of the density profile) remains rigid throughout its motion [1]. These two features are closely related to each other.

We are interested in relativistic versions of the HO. We confine ourselves to one space dimension throughout this paper. We seek potentials for the Dirac equation such that feature (i) mentioned above holds for the positive-energy states. We expect that such potentials also exhibit feature (ii) in a good approximation. Regarding their behavior under the Lorentz transformation, there are three types of potentials for the Dirac equation: vector, scalar, and pseudoscalar. By the vector type we actually mean the zeroth component of a vector (such as the Coulomb potential). Relativistic versions of the HO can be constructed with potentials of the scalar and pseudoscalar types, but not with a potential of the vector type. This can be done by means of the ''inverse scattering method.'' For a set of given energy levels, the method enables us to determine a potential that reproduces the set of energy levels.

One can first construct a potential by assuming N equally spaced energy levels and then letting $N\rightarrow\infty$. In practice, however, one stops at a large but finite value of N. For the set of assumed N energy levels, we take those of positive energies. If we do so, for the Lorentz scalar and pseudoscalar potentials, the negative-energy levels also become equally spaced. However, there is a gap between the lowest positive energy and the highest negative energy. For this gap we choose a value different from the gap between two adjacent positive- (or negative-) energy levels. In this sense we require feature (i) separately for the positive- and negative-energy levels. In a certain situation of the scalar potential a complication arises regarding the presence of a zero-energy bound state (''zero mode'').

We show how a relativistic HO of the Lorentz scalar type can be constructed explicitly in Sec. II. In Sec. III we examine the pseudoscalar type. We give explicit illustrations of HO potentials in Sec. IV. We also examine the time-dependent behavior of a wave packet in the potentials. A summary is given in Sec. V. In the Appendix we point out that a HO-like potential of the vector type allows no bound state.

II. SCALAR POTENTIAL

We follow Ref. [2] in which some supersymmetry (SUSY) aspects of the Dirac equation with a Lorentz scalar potential in one dimension were discussed. Example D of that paper, in particular, gives a prescription for the inverse problem (in which a potential that reproduces a set of given energy levels is constructed). The method can be summarized as follows. We use the same notation as in Ref. [2]: $c=\hbar=1$. The Dirac equation that we consider is

$$H\psi(x)=E\psi(x), \quad H=\alpha p+\beta[m+S(x)], \tag{1}$$

where $p=-i\partial/\partial x$, m is the rest mass of the particle, and $S(x)$ is the scalar potential. Since m and $S(x)$ are both scalar quantities, the separation between m and $S(x)$ is actually arbitrary. The wave function ψ has two components. We denote the upper (lower) component ψ_1 (ψ_2). For the Dirac matrices α and β, we use the 2×2 Pauli matrices $\alpha=\sigma_y$ and $\beta=\sigma_x$. With this choice of α, the wave functions for stationary states can be taken as real. Note that $\sigma_z\psi(x)$ satisfies Eq. (1) with E replaced by $-E$. Hence there is symmetry between positive and negative energies. The orthogonality between the states of $\pm|E|$ leads to $\int_{-\infty}^{\infty}\psi_1^2(x)dx=\int_{-\infty}^{\infty}\psi_2^2(x)dx=\frac{1}{2}$.

Equation (1) can be reduced to the following SUSY pair of Schrödinger equations [3,4]:

*Author to whom correspondence should be addressed. FAX: 81 75 705 1914. Electronic address: toyama@ksuvx0.kyoto-su.ac.jp

$$H_i\psi_i=\left(\frac{p^2}{2m}+U_i\right)\psi_i=\epsilon\psi_i, \quad \epsilon=\frac{E^2-m^2}{2m}, \tag{2}$$

where $i=1$ or 2, and

$$U_i(x)=\frac{1}{2m}\left((m+S)^2-m^2\mp\frac{dS}{dx}\right). \tag{3}$$

The double sign of Eq. (3) is $-(+)$ for $i=1$ (2).

Consider the Dirac equation for $E=0$, i.e., $\epsilon=-m/2$. Let the upper (lower) component of a solution of this equation be ϕ_1 (ϕ_2). Then ϕ_i satisfies

$$\left(-\frac{1}{2m}\frac{d^2}{dx^2}+U_i\right)\phi_i=-\frac{m}{2}\phi_i. \tag{4}$$

If S and ϕ_i are related by

$$m+S(x)=\mp\frac{d}{dx}\ln\phi_i(x), \tag{5}$$

Eq. (2) together with Eq. (3) is satisfied. The reason why we are interested in Eqs. (4) and (5) is the following. For an assumed set of energy levels, we can determine U_i by means of the Kay-Moses method [5,6]. Then one may try to determine S by solving Eq. (3) for unknown S. This is not easy. However, ϕ_i can be easily determined as a scattering wave function for the Kay-Moses potential. Once ϕ_i is found, S immediately follows from Eq. (5). It is sufficient to use $i=1$ or 2. If the lowest eigenvalue of Eq. (2) for $i=1$ is above $-m/2$, then we can choose ϕ_1 such that it has no node. This is true in all the cases that we are going to consider. Then Eq. (5) furnishes a nonsingular potential $S(x)$. For the $S(x)$ so determined, the partner potential U_2 can be determined by Eq. (3). Regarding the relative sign between the asymptotic values of $S(\infty)$ and $S(-\infty)$, we classify $S(x)$ into two types, I and II. If $S(\infty)$ and $S(-\infty)$ are of the same sign, we say that $S(x)$ is of type I. If they are of opposite signs, $S(x)$ is said to be of type II. Types I and II are what we referred to as nontopological and topological, respectively, in Ref. [2].

We are now ready to write down the inverse problem prescription. Assume a sequence of positive-energy eigenvalues of H, $E_1<E_2<E_3<\cdots<E_N$. The following prescription works for any E_n's as long as they are nonnegative. For the HO that we are interested in, we assume the equally spaced sequence

$$E_n=E_1+(n-1)\omega, \tag{6}$$

where $n=1,2,3,\ldots,N$ and $\omega>0$ is a constant. Ideally N should be ∞, but in practice we take it to be finite but large.

Define ϵ_n's and κ_n's such that

$$\epsilon_n=-\frac{\kappa_n^2}{2m}=\frac{E_n^2-m^2}{2m}. \tag{7}$$

Then, following Kay and Moses [5–7], we can find the potential $U_1(x)$ such that the Schrödinger equation (2) for $i=1$ has eigenvalues ϵ_n. Actually, there is an infinite family of such potentials. For such a U_1 we can find ϕ_1. When the ϕ_1 is found, the potential $S(x)$ that leads to the assumed energy eigenvalues of the Dirac equation is given by Eq. (5).

A prescription for the above senario goes as follows. Introduce an $N\times N$ matrix $\hat{A}(x)$ with its marix elements

$$\hat{A}_{ij}(x)=(A_iA_j)^{1/2}\frac{e^{(\kappa_i+\kappa_j)x}}{\kappa_i+\kappa_j}, \tag{8}$$

where A_i ($i=1,2,\ldots,N$) are arbitrary positive constants. The potential $U_1(x)$ is given by

$$U_1(x)=-\frac{1}{m}\frac{d^2}{dx^2}\ln\{\det[I+\hat{A}(x)]\}, \tag{9}$$

where I stands for the $N\times N$ unit matrix. Equation (2) with the above U_1 has the scattering state solution

$$\chi(k,x)=\left(1+\sum_{i=1}^{N}\frac{\sqrt{A_i}g_i(x)e^{\kappa_i x}}{ik+\kappa_i}\right)e^{ikx}, \tag{10}$$

where $k^2=E^2-m^2$ and $g_i(x)$'s are defined by the N linear algebraic equation [8]

$$\sum_{j=1}^{N}[\delta_{ij}+\hat{A}_{ij}(x)]g_j(x)+\sqrt{A_i}e^{\kappa_i x}=0. \tag{11}$$

If we set $k=im$, $\chi(im,x)$ and $\chi(im,-x)$ satisfy Eq. (2) with $\epsilon=-m/2$. Hence the ϕ_1 of Eq. (4) can be taken as an arbitrary linear combination of $\chi(im,x)$ and $\chi(im,-x)$. If we take $\chi(im,x)$ or $\chi(im,-x)$ for ϕ_1, then the ensuing $S(x)$ becomes type I. If we combine $\chi(im,x)$ and $\chi(im,-x)$, we obtain an $S(x)$ of type II.

Let us first take type I (nontopological). Assume that

$$\phi_1(x)=\chi(im,x). \tag{12}$$

For an arbitrary choice of A_i's, $U_1(x)$ and $S(x)$ have no symmetry in general. If we choose A_i's as

$$\frac{A_i}{2\kappa_i}=\prod_{j\neq i}\frac{\kappa_i+\kappa_j}{|\kappa_i-\kappa_j|}, \tag{13}$$

$U_1(x)$ becomes symmetric, i.e., an even function of x. In this case, however, the $S(x)$ that ensues is not symmetric. A more interesting choice of A_i is

$$\frac{A_i}{2\kappa_i}=\left(\frac{m-\kappa_i}{m+\kappa_i}\right)^{1/2}\prod_{j\neq i}\frac{\kappa_i+\kappa_j}{|\kappa_i-\kappa_j|}, \tag{14}$$

which leads to $U_1(x)=U_2(-x)$ and symmetric $S(x)$. For the illustrations that we present in Sec. III, we use Eq. (14) for type I.

For type II (topological), we can assume that

$$\phi_1(x)=\chi(im,x)+\chi(im,-x). \tag{15}$$

This $\phi_1(x)$ is an even function of x. Then $m+S(x)$ becomes an odd function of x. The $U_1(x)$ and $U_2(x)$ both become even functions of x, irrespective of the choice of A_i's. In the illustrations of Sec. III we use Eq. (13).

Now that the potential $S(x)$ is determined and the assumed positive-energy eigenvalues are reproduced, one naturally asks if the $S(x)$ leads to any other eigenvalues of H. It can be shown that there are no other positive-energy bound states [2]. There is symmetry between positive- and negative-energy spectra. The negative-energy eigenvalues are $-E_1>-E_2>-E_3>\cdots>-E_N$. The corresponding wave functions are, as we pointed out below Eq. (1), given by $\sigma_z\psi$. If $S(x)$ is type I, there is no bound state of $E=0$.

If $S(x)$ is type II, however, there is a bound state with $E=0$ [9]. The wave function of the bound state of $E=0$ is given by

$$\psi_1(x)=0, \quad \psi_2(x)=N_0\exp\left(\int_0^x [m+S(x)]dx\right), \quad (16)$$

where N_0 is an appropriate normalization constant. It is understood that $m+S(x)<0$ (>0) for $x\to\infty$ $(-\infty)$. It can be shown that $\psi_2(x)=1/\phi_1(x)$, where $\phi_1(x)$ is that of Eq. (15). Alternatively, one can include $E=0$ in the set of assumed energy levels and determine $\psi_2(x)$ as one of the Kay-Moses wave functions. In the actual calculations we found this alternative method more straightforward. This concludes the prescription of the inverse method for the Lorentz scalar potential.

Before ending this section let us mention special cases with $m=0$. Assume that $S(x)$ is an infinite square well potential of type I:

$$S(x)=\begin{cases}\infty & \text{if } |x|>a\\ 0 & \text{if } |x|<a.\end{cases} \quad (17)$$

Then we obtain

$$E=\pm\frac{(2n-1)\pi}{4a}, \quad (18)$$

where $n=1,2,\ldots$. The entire (positive- and negative-) energy spectrum is equally spaced. The reason why there is only one value of energy separation is that the model contains only one parameter with dimension, i.e., a.

For an infinite potential of type II,

$$S(x)=\begin{cases}\mp\infty & \text{if } |x|>a\\ 0 & \text{if } |x|<a,\end{cases} \quad (19)$$

where the double sign is minus (plus) for $x>0$ $(x<0)$, we obtain

$$E=\frac{n\pi}{2a}, \quad (20)$$

where $n=0,\pm1,\pm2,\ldots$. All energy levels are equally spaced, including the zero mode.

III. PSEUDOSCALAR POTENTIAL

The Dirac equation that we consider is

$$H\psi(x)=E\psi(x), \quad H=\alpha[p-i\beta f(x)]+\beta m. \quad (21)$$

Note that $\psi^\dagger\alpha\beta\psi$ is a pseudoscalar quantity. For the Dirac matrices α and β, we use $\alpha=\sigma_y$ and $\beta=\sigma_z$. This β is different from what we used in Sec. II. Again let the upper (lower) component of ψ be ψ_1 (ψ_2). Then Eq. (21) can be manipulated into the SUSY pair of the Schrödinger equations

$$H_i\psi_i=\left(\frac{p^2}{2m}+W_i\right)\psi_i=\epsilon\psi_i, \quad \epsilon=\frac{E^2-m^2}{2m}, \quad (22)$$

$$W_i(x)=\frac{1}{2m}\left(f^2\mp\frac{df}{dx}\right), \quad (23)$$

where $i=1$ or 2 and the double sign in Eq. (23) is $-(+)$ for $i=1$ (2). It is known that ϵ is non-negative. Consider the Dirac equation for $E=m$ and $\epsilon=0$. Let the upper component of the wave function be ϕ_1. The ϕ_1 satisfies

$$-\frac{1}{2m}\frac{d^2\phi_1}{dx^2}+W_1\phi_1=0. \quad (24)$$

The ϕ_1 and f are related by

$$f(x)=-\frac{d}{dx}\ln\phi_1(x). \quad (25)$$

In the special case of $f(x)=m\omega x$, we obtain

$$W_i(x)=\frac{1}{2}(m\omega^2x^2\mp\omega), \quad (26)$$

where the double sign is the same as that of Eq. (23). This case is known as the Dirac oscillator [10–12]. The SUSY Schrödinger equations and hence the Dirac equation are analytically solvable. The eigenvalues of H_i are equally spaced, but those of H are not. This is not the HO that we are interested in now. As shown in Refs. [11,12] in detail, the behavior of a wave packet in the Dirac oscillator potential is very different from that of Schrödinger's coherent wave packet.

Now assume a sequence of positive-energy eigenvalues of H, $E_1<E_2<\cdots<E_N$. The E_i's can take any positive values not smaller than m. In the actual calculation, we take the equally spaced positive-energy levels of Eq. (6). Assume that $W_1(x)$ is given by

$$W_1(x)=\frac{\kappa_1^2}{2m}+U_1(x), \quad (27)$$

where $U_1(x)$ is that of Eq. (9). Then Eq. (22) for ψ_1 has N bound states with N eigenvalues [13]:

$$\epsilon_i=\frac{E_i^2-m^2}{2m}=\frac{\kappa_1^2-\kappa_i^2}{2m}. \quad (28)$$

There are no other positive-energy bound states. For the assumed eigenvalues of H, i.e., E_i's, the κ_i's can be chosen arbitrarily as long as they are related to the E_i's through Eq. (28). Apart from a constant factor, ϕ_1 can be taken as

$$\phi_1(x)=\chi(i\kappa_1,x), \quad (29)$$

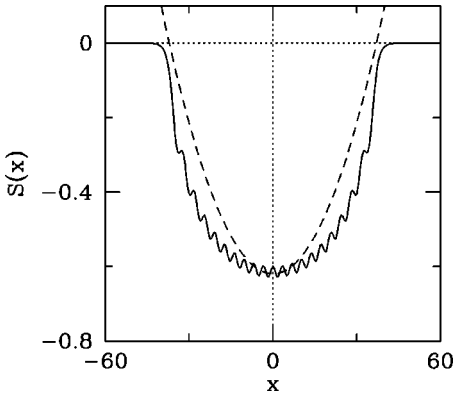

FIG. 1. The solid line shows the scalar HO potential $S(x)$, type I, constructed in Sec. IV. Units are such that $c=\hbar=m=1$. The dashed line shows the nonrelativistic HO potential $\frac{1}{2}m\omega^2x^2$ with $m=1$ and $\omega=\Delta E=0.03$.

where $\chi(i\kappa_1,x)$ is the $\chi(k,x)$ of Eq. (10) with $k=i\kappa_1$. Now that the ϕ_1 is known, the potential function $f(x)$ can be determined by Eq. (25). Then we can go on to determine the SUSY partner W_2. About the symmetry of W_1 and W_2, let us choose A_i's according to Eq. (13) so that $W_1(x)$ is symmetric. It then follows that $f(x)$ is an odd function of x and $W_2(x)$ an even function of x. Note that there was an additional parameter λ in Ref. [13]. We have chosen $\lambda=1$ so that $U_2(x)$ becomes symmetric.

The negative-energy eigenvalues are $-E_2>-E_3>\cdots$. These are all less than $-m$. Note also that there is no bound state with $-E_1$. Let us examine the relation between the wave functions of a pair of bound states of energies E_n and $-E_n<0$. Let the upper (lower) component of the normalized wave function of the positive-energy state be ψ_1 (ψ_2) and those of the negative-energy state φ_1 (φ_2). Then we find that $\psi_i\propto\varphi_i$ for both of $i=1$ and 2. This can be shown by operating σ_x on the Dirac equation (21) from the left and then replacing $f(x)$ with $-f(x)$. Note that when $f(x)\rightarrow -f(x)$, $i=1\leftrightarrow 2$ in Eqs. (22) and (23). It is convenient to introduce functions χ_i such that

$$\chi_i(x)\propto\psi_i(x), \quad \int_{-\infty}^{\infty}\chi_i^2(x)dx=1. \tag{30}$$

It then follows from Eq. (21) that the components of the wave functions of a pair of positive- and negative-energy states (of $\pm E_n$) can be expressed as

$$\psi_i(x)=c_i\chi_i(x), \quad \varphi_i(x)=c_i'\chi_i(x), \tag{31}$$

where

$$c_i=\sqrt{\frac{E_n\pm m}{2E_n}}, \quad c_i'=\pm\sqrt{\frac{E_n\mp m}{2E_n}}. \tag{32}$$

For the double sign we take the upper (lower) one for $i=1$ (2). Finally, if we set $m=0$, the model becomes equivalent to that of the scalar potential of type II with $m=0$, which we discussed at the end of Sec. II.

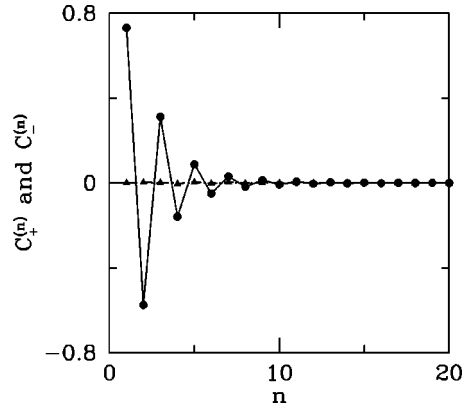

FIG. 2. Expansion coefficients of Eq. (33) for the wave packet in the scalar HO potential of type I. Units are such that $c=\hbar=m=1$. The dots are for $C_+^{(n)}$ and the triangles are for $C_-^{(n)}$.

IV. HO POTENTIALS: ILLUSTRATIONS

In this section we explicitly construct scalar HO potentials of types I and II and also a pseudoscalar HO potential. We then examine the behavior of wave packets in the potentials. We will show eleven figures, four each for types I and II of the scalar, and three for the pseudoscalar. We set $m=1$ throughout this section.

For the type I scalar, we assume the lowest positive energy $E_1=0.4$, the energy separation $\Delta E=\omega=0.03$, and the number of positive-energy levels $N=20$. In addition, there are 20 negative-energy states. In somewhat similar but nonrelativistic inverse problems, Schonfeld *et al.* took $N=8$ and Asthan and Kamal took $N=5$ [6]. With $N=20$ we obtain far better convergence. Figure 1 shows $S(x)$. It fluctuates. This is because N is finite. The fluctuations will disappear as $N\rightarrow\infty$. The dashed line shows the nonrelativistic HO potential $\frac{1}{2}m\omega^2x^2$ with $m=1$ and $\omega=0.03$. The relativistic HO potential is flatter at the bottom than its nonrelativistic counterpart. If we let $m\rightarrow 0$ and $N\rightarrow\infty$, $S(x)$ approaches the infinite square well potential of Eq. (17).

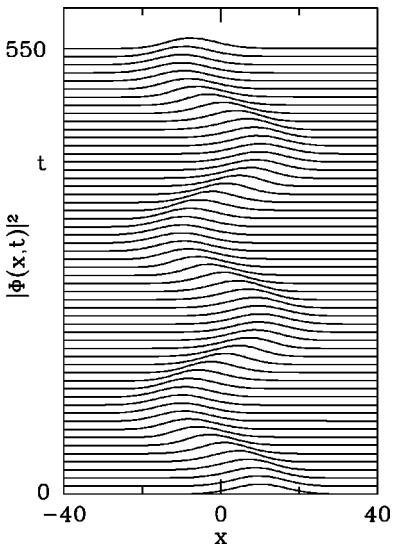

FIG. 3. Density profile of the wave packet as a function of x and t in the scalar HO potential of type I. Units are such that $c=\hbar=m=1$.

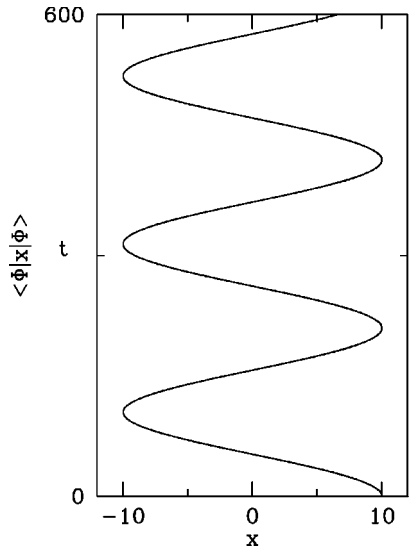

FIG. 4. Comparison of the motion of the centroid $\langle x\rangle$ (solid line) in the scalar HO potential of type I and $x_0\cos\omega t$, where $x_0=10$ and $\omega=\Delta E=0.03$ (dotted line). The two lines are almost indistinguishable. Units are such that $c=\hbar=m=1$.

For the wave packet, we start (at $t=0$) with the lowest positive-energy state that is shifted such that its center is at $x_0=10$. The time-dependent wave function $\psi(x,t)$ of the wave packet can be written as a superposition of stationary states

$$\psi(x,t)=\sum_n C_+^{(n)}\psi_+^{(n)}(x,t)+\sum_n C_-^{(n)}\psi_-^{(n)}(x,t), \quad (33)$$

where the subscript $+$ or $-$ refers to the sign of the energy. The coefficients are all real. In principle, we should include continuum states. Figure 2 shows the coefficients. With $N=20$ the expansion has converged very well, which means that the continuum contribution is negligible. Figure 3 shows the density profile of the wave packet as a function of x and t. This is very much like that of Schrödinger's nonrelativistic coherent wave packet. The shape of the wave packet is well (but not exactly) maintained. Figure 4 compares the motion of the centroid $\langle x\rangle$ of the wave packet and $x_0\cos\omega t$. These two are almost indistinguishable. The centroid moves smoothly. *Zitterbewegung* is not noticeable.

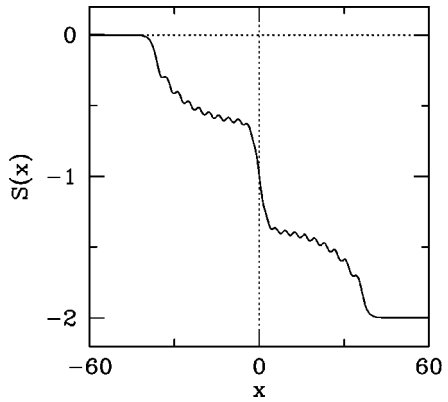

FIG. 5. Scalar HO potential $S(x)$, type II, constructed in Sec. IV. Units are such that $c=\hbar=m=1$.

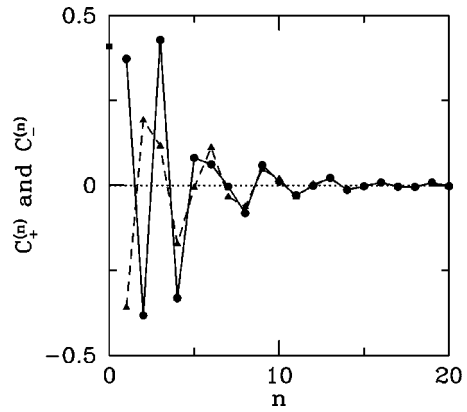

FIG. 6. Expansion coefficients for the wave packet in the scalar HO potential of type II. The dots are for $C_+^{(n)}$ and the triangles are for $C_-^{(n)}$. The coefficient for the zero mode $(n=0)$ is shown with a square. Units are such that $c=\hbar=m=1$.

For type II we assume the same positive- and negative-energy states as we did for type I. In addition, there is a zero mode. Figure 5 shows $S(x)$. As $x\to\pm\infty$, $m+S(x)\to\mp\kappa_1=\mp m$. We construct a wave packet in the same way as for type I, but we include the zero mode. Figure 6 shows the expansion coefficients. Note that the amplitude for the zero mode $(n=0)$ is substantial. Figure 7 shows the density profile of the wave packet as a function of x and t. The shape of the wave packet is not well maintained. This is probably due to the admixture of the zero mode that does not oscillate. Figure 8 compares the motion of the centroid $\langle x\rangle$ and $x_0\cos\omega t$. These two are fairly close to each other except that the centroid oscillates with small amplitude. By magnifying the graph, we find that the period of oscillations is approximately 7. These oscillations can be interpreted as *Zitterbewegung* that is due to the admixture of negative-energy states. (See the last paragraph of this section.)

Let us now turn to the pseudoscalar case. We again assume the lowest positive energy $E_1=0.4$, the energy separation $\Delta E=\omega=0.04$, and the number of positive-energy levels

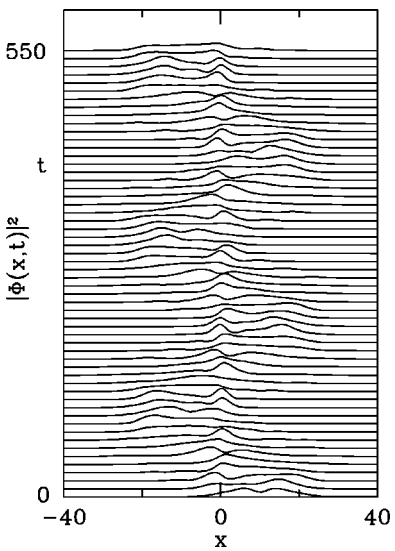

FIG. 7. Density profile of the wave packet as a function of x and t in the scalar HO potential of type II. Units are such that $c=\hbar=m=1$.

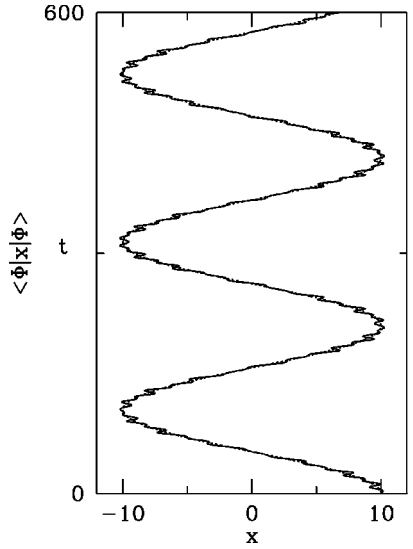

FIG. 8. Comparison of the motion of the centroid $\langle x \rangle$ (solid line) in the scalar HO potential of type II and $x_0 \cos \omega t$, where $x_0 = 10$ and $\omega = \Delta E = 0.03$ (dotted line). Units are such that $c = \hbar = m = 1$.

$N = 20$. The κ_1 of Eq. (28) can be chosen arbitrarily, but the degree of localization of the wave packet is sensitive to κ_1. We take $\kappa_1 = 1.46$. We have chosen this value of κ_1 so that the wave packet is well localized. Figure 9 shows $f(x)$. As $x \to \pm\infty$, $f(x) \to \pm\kappa_1$.

We construct a wave packet in the same way as in Sec. III except that we choose $x_0 = 5$ this time. Figure 10 shows the expansion coefficients. With $N = 20$ the expansion has converged well. (The stationary state of energy $-E_1$ is absent.) Figure 11 shows the density profile of the wave packet as a function of x and t. This is again very much like that of Schrödinger's nonrelativistic coherent wave packet and the shape of the wave packet is well (but not exactly) maintained. The centroid $\langle x \rangle$ closely follows $x_0 \cos \omega t$, where $\omega = \Delta E$. The centroid exhibits slight *Zitterbewegung* with a period of about 3.

In order to confirm that the small oscillations are a manifestation of *Zitterbewegung*, we repeated the calculation for the pseudoscalar potential in the Foldy-Wouthuysen representation [14,12]. In this representation the positive- and negative-energy states are separated. The wave functions of

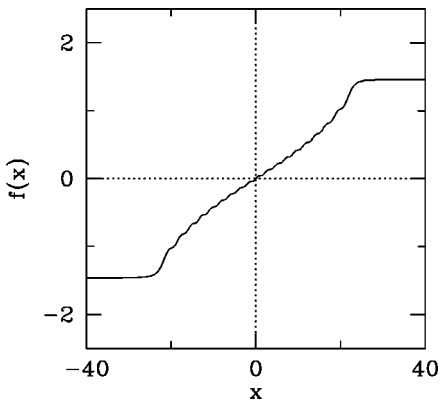

FIG. 9. Pseudoscalar HO potential $f(x)$ constructed in Sec. IV. Units are such that $c = \hbar = m = 1$.

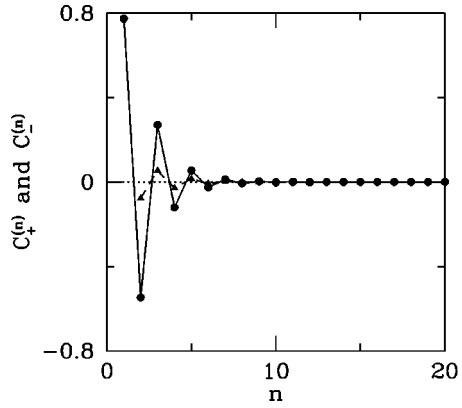

FIG. 10. Expansion coefficients for the wave packet in the pseudoscalar HO potential. The dots are for $C_+^{(n)}$ and the triangles are for $C_-^{(n)}$. Units are such that $c = \hbar = m = 1$.

the positive-energy states consist of only the upper components. We found that the trajectory of the centroid in that representation is indeed smooth and indistinguishable from $x_0 \cos \omega t$. For the scalar potenial it is difficult to work out the Foldy-Wouthuysen representation, but we believe that the oscillations that we have seen in Fig. 8 are due to *Zitterbewegung*.

V. SUMMARY

We constructed relativistic versions of the HO potential for the Dirac equation in one dimension. They are characterized by the positive-energy levels that are equally spaced. As far as we know, this is the first time that such potentials are presented. We did this by means of the ''inverse scattering method.'' We considered Lorentz scalar and pseudoscalar potentials. If the potential is (the zeroth component of) a Lorentz vector, it is not possible to construct a HO potential. There are two types of the scalar potential, type I (nontopological) and type II (topological). The relativistic HO of

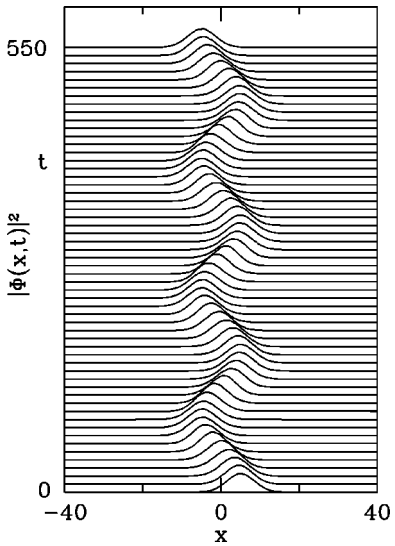

FIG. 11. Density profile of the wave packet as a function of x and t in the pseudoscalar HO potential. Units are such that $c = \hbar = m = 1$.

the type I scalar is a very natural extension of the nonrelativistic HO.

We examined the behavior of a wave packet in the relativistic HO potentials. We started with the wave function that was obtained by shifting the state of the lowest positive energy to a certain position. In the type I scalar and pseudoscalar potentials, the wave packet behaves much like Schrödinger's coherent wave packet. In the scalar potential of type II, the behavior of the wave packet is somewhat complicated. As we discussed, this is related to the presence of the zero mode. The wave packet exhibits *Zitterbewegung*, in particular, in the type II scalar and the pseudoscalar cases. If we take the Foldy-Wouthuysen representation, however, the *Zitterwebegung* should disappear. We confirmed this for the pseudoscalar HO potential.

ACKNOWLEDGMENTS

This work was supported by the Ministry of Education of Japan and the Natural Sciences and Engineering Research Council of Canada.

APPENDIX

We show why it is not possible to have a HO potential of the Lorentz vector type. Recall feature (i) that we require for a HO potential. (See the beginning of Sec. I.) The spectrum of the HO potential consists of an infinite number of discrete states and no continuum states.

Consider the Dirac equation with a potential that is the zeroth component of a Lorentz vector,

$$H\psi(x)=E\psi(x), \quad H=\alpha p+\beta m+V(x). \tag{A1}$$

Let us start with $V(x)$ defined by

$$V(x)=\begin{cases} \frac{1}{2}m\omega^2x^2 & \text{if } |x|<a \\ V(a)=\frac{1}{2}m\omega^2a^2 & \text{if } |x|>a. \end{cases} \tag{A2}$$

In the region of $|x|>a$ where the potential is a constant, the wave function is of the form of e^{ikx} or $e^{\pm\kappa x}$ depending on the sign of $[E-V(a)]^2-m^2$. A bound state can be found only if its energy E is in the range of $[E-V(a)]^2-m^2<0$, i.e.,

$$m+V(a)>E>-m+V(a). \tag{A3}$$

There exist continuum states with E that is outside the range of Eq. (A3). Therefore, when we keep a finite, we can have discrete states (but only finite in number). In addition, there are continuum states. If we let $a\to\infty$, the energy of a bound state (if any) becomes infinite. This implies that if $V(x)=\frac{1}{2}m\omega^2x^2$ in the entire space, the Hamiltonian with the $V(x)$ has no finite, discrete eigenvalues. It is clear that in either case of finite or infinite a, we cannot have feature (i), which characterizes the HO potential.

In the above we assumed a specific form of Eq. (A2) for $V(x)$, but exactly the same situation obtains when $V(x)$ is replaced by any confining potential such that $|V(x)|\to\infty$ as $|x|\to\infty$. Such a $V(x)$ allows no discrete eigenstates. The potential may try to confine a particle, but the particle will eventually leak out to infinity. This must have been known to many people, in particular to those who considered models of quark confinement. Let us also add that, as far as we know, the inverse scattering problem is possible only for the Lorentz scalar and pseudoscalar potentials, but not for a vector-type potential. This is probably related to the ''impossibility'' of the HO potential in the vector case.

[1] E. Schrödinger, Naturwissenshaften **14**, 664 (1926); Ann. Phys. (Leipzig) **79**, 489 (1926).
[2] Y. Nogami and F. M. Toyama, Phys. Rev. A **47**, 1708 (1993).
[3] F. Cooper, A. Khare, R. Musto, and A. Wipf, Ann. Phys. (N.Y.) **187**, 1 (1987).
[4] For SUSY of nonrelativistic quantum mechanics see, e.g., R. Dutt, A. Khare, and U. P. Sukhatme, Am. J. Phys. **56**, 163 (1988).
[5] I. Kay and H. E. Moses, J. Appl. Phys. **27**, 1503 (1956).
[6] J. F. Schonfeld, W. Kwong, J. L. Rosener, C. Quigg, and H. B. Thacker, Ann. Phys. (N.Y.) **128**, 1 (1980); P. Asthana and A. N. Kamal, Z. Phys. C **19**, 37 (1983).
[7] F. M. Toyama, Y. Nogami, and Z. Zhao, Phys. Rev. A **47**, 897 (1993).
[8] Equation (10) corresponds to Eq. (3.20) of Ref. [2]. In the latter the inhomogeneous term $\sqrt{A_i}e^{\kappa_i x}$ was inadvertently dropped. Also, the right-hand side of Eq. (3.16) of Ref. [2] should be multiplied by $1/2m$.
[9] R. Jackiw and C. Rebbi, Phys. Rev. D **13**, 3398 (1976); F. A. B. Coutinho, Y. Nogami, and F. M. Toyama, Am. J. Phys. **56**, 904 (1988).
[10] D. Ito, K. Mori, and J. Carriere, Nuovo Cimento A **51**, 119 (1967); P. A. Cook, Lett. Nuovo Cimento **1**, 419 (1971); M. Moshinsky and A. Szczepaniak, J. Phys. A **22**, L817 (1989); M. Moreno and A. Zentella, *ibid.* **22**, L82 (1989).
[11] Y. Nogami and F. M. Toyama, Can. J. Phys. **74**, 114 (1996).
[12] F. M. Toyama, Y. Nogami, and F. A. B. Coutinho, J. Phys. A **30**, 2585 (1997).
[13] Y. Nogami and F. M. Toyama, Phys. Rev. A **57**, 93 (1998).
[14] L. L. Foldy and S. A. Wouthuysen, Phys. Rev. **78**, 29 (1950).